Carbon 218 (2024) 118744

Contents lists available at ScienceDirect

Carbon

journal homepage: www.elsevier.com/locate/carbon

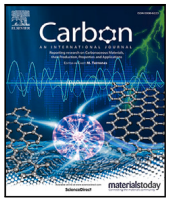

Research paper

Few-layer graphene as an 'active' conductive additive for flexible aqueous supercapacitor electrodes

R.E. Williams [a], S. Sukumaran [a,b], Q. Abbas [a,c], M.R.C. Hunt [a,*]

[a] Department of Physics, Durham University, Durham, DH1 3LE, United Kingdom
[b] Department of Materials, Imperial College, London, SW7 2AZ, United Kingdom
[c] School of Engineering, Computing and Physical Sciences, University of the West of Scotland, Paisley, PA1 2BE, United Kingdom

ARTICLE INFO

Keywords:
Supercapacitor
EDLC
Few-layer graphene
Conductive additive

ABSTRACT

We demonstrate that few layer graphene (FLG), formed by high-shear exfoliation into an aqueous suspension, can be successfully employed as an 'active' conductive additive in flexible activated carbon-based aqueous electric double layer capacitor (supercapacitor) electrodes if introduced by a novel 'vacuum infiltration' technique. The effectiveness of the FLG can be optimised by tailoring its size distribution and loading. It is found that best performance is achieved using FLG with the broadest size distribution and, moreover, that the larger size distribution is effective over the broadest range of loading. With optimum size distribution and loading, FLG is shown to outperform a commercial carbon black conductive additive (Timcal C65). Electrodes containing 8 wt% infiltrated FLG have an equivalent series resistance (ESR) of $1.3 \pm 0.4\ \Omega$, and a specific capacitance of 142.3 ± 0.1 F g^{-1} over a voltage window of 1.2 V, compared with an ESR of $3 \pm 1\ \Omega$ and a specific capacitance of 96.81 ± 0.02 F g^{-1} for equivalent electrodes produced with an optimal loading of carbon black additive. As a result, the specific energy density of electric double layer capacitors (EDLCs) produced with a vacuum infused FLG additive is demonstrated to be an average of $47 \pm 3\%$ superior to those containing carbon black measured at similar power densities. In contrast to vacuum infiltration, direct mixing of FLG suspension into the electrodes is found to be ineffective, resulting in limited improvement relative to electrodes without conductive additive, the reasons for which are discussed.

1. Introduction

Electric double layer capacitors (EDLCs) – often termed supercapacitors – attract considerable interest for sustainable energy storage due to their long cycle life and high specific power density in comparison with current battery technologies [1,2]. The characteristics of EDLCs make them of particular value for rapid delivery/harvesting of energy, for example in electric vehicle acceleration/braking, for stationary applications such as smoothing fluctuations from renewable energy generation, and for power grid regulation [2]. Moreover, the longevity of EDLCs, which results from the purely physical storage of charge [3], coupled with the use of Earth-abundant and readily recyclable materials in their construction avoids many of the potentially unsustainable aspects of the current generation of battery technologies.

Activated carbon is often favoured as an electrode material for EDLCs due to its low cost, high specific surface area (SSA), and controlled hierarchical pore size distribution, which allow for high specific capacitances [1,4,5]. Unfortunately, in the absence of conductive additives, activated carbon electrodes are excessively resistive, leading to poor measured capacitance at high charge/discharge rates, and limiting the maximum power output of the device [6]. Carbon black is widely used as an additive, substantially improving electrode conductivity, however, its limited contribution to the double layer capacitance means this often comes at the expense of reducing the overall specific capacitance (C_{sp}) of an electrode.

A variety of carbon materials, including carbon nanotubes (CNTs), carbon fibres, carbon onions, expanded graphite, and graphite nanoflakes have been investigated as alternative conductive additives [7–10]. Of these, CNTs have been shown to offer the best performance [7,8]. However, CNTs are impractical as a replacement to carbon blacks, due to both their extremely high cost and serious concerns with regard to their safety [11].

Pandolfo et al. compared carbon black with micrographite flakes as conductive additives [10] and found that carbon black has a resistivity similar to activated carbon (~40 mΩ cm), four times that of the graphite flakes. In spite of this, the carbon black was found to be a superior conductive additive. This was attributed to the structure of

* Corresponding author.
E-mail address: m.r.c.hunt@durham.ac.uk (M.R.C. Hunt).

https://doi.org/10.1016/j.carbon.2023.118744
Received 1 November 2023; Received in revised form 11 December 2023; Accepted 14 December 2023
Available online 16 December 2023

the carbon black, which consists of agglomerations of small (~20 nm) particles, allowing it to more effectively fill voids and improve conductivity between activated carbon particles, indicating the importance of the dimensions of the additive.

The high conductivity and specific surface area of graphene has made it a promising material for EDLCs [12]. When used as a standalone electrode material, capacitance is limited by restacking of the graphene sheets, reducing available surface area. However, graphene-based materials have been explored as conductive additives with positive results [13–15]. For example, electrodes containing 1 wt% graphene quantum dots were found to have comparable ESR and enhanced C_{sp} relative to those containing 10 wt% carbon black [14].

In this work we use few-layer graphene (FLG) platelets, produced by high-shear exfoliation [16] into an aqueous suspension stabilised by a surfactant [17,18], as an *active* conductive additive (i.e., one which contributes to the double layer capacitance) in activated carbon EDLC electrodes. By using water, rather than organic solvents, as the liquid phase the production of FLG can be considered environmentally benign. Moreover, the harsh environmentally unfriendly treatments required for the production of analogous materials such as graphene oxide (GO) from which the conductive reduced graphene oxide (rGO) can be produced [15] are avoided. Hence, shear exfoliation into aqueous suspension is an attractive route to produce FLG platelets for use in supercapacitor applications [19].

Direct mixing of the FLG suspension into activated carbon with a polytetrafluoroethylene (PTFE) binder during electrode fabrication is examined and found to produce mediocre results, leading to the development of a novel 'vacuum infiltration' technique. The performance gain for FLG-infiltrated electrodes is examined, in particular the influence of FLG size distribution and loading on electrode performance. To reliably determine the effectiveness of vacuum infiltration of FLG in improving EDLC properties, the results of electrochemical characterisation were compared with those from 'baseline' electrodes analogously produced with and without a commercially-available carbon black conductive additive.

2. Experimental section

2.1. Preparation of FLG

Few layer graphene was produced by liquid phase high-shear exfoliation of natural graphite flakes (Alfa Aesar) into ultra-high purity (UHP) water (15 MΩ cm) with Triton X-100 surfactant (1.25 g per litre) obtained from Sigma-Aldrich. Exfoliation employed a Silverson L5M high shear mixer operating at a shear speed of 9000 rpm, corresponding to a shear rate, $\dot{\gamma} \approx 10^5$ s^{-1}, for a duration of 4 h. The resulting mixture was subsequently processed under three different conditions: a 'moderate' centrifugation at 2000 rpm for 20 minutes to produce material labelled 'mFLG'; a 'high' centrifugation at 7500 rpm for 1 h to produce material labelled 'hFLG'; and a third batch was left uncentrifuged, labelled 'uFLG'. Centrifugation was performed with an Eppendorf 7500 centrifuge using 50 ml centrifuge tubes. After centrifuging, the top 40 ml of the suspension was pipetted off to either produce 'FLG paper', or to be incorporated into activated carbon electrodes as described below.

2.2. Preparation of electrodes and FLG paper

Supelco Activated carbon (AC) was obtained from Sigma-Aldrich and used with no pretreatment. 60 wt% PTFE in water (Sigma-Aldrich) was used as a binder, and where relevant, Timcal Super C65 carbon black was used as a conductive additive. To produce activated carbon electrode material without any conductive additive, 95 wt% activated carbon and 5 wt% PTFE were mixed with around 1 ml of ethanol until a cohesive paste was formed. This was then rolled out thinly using 75 μm stainless steel shims as a thickness guide and dried overnight, resulting in electrode material of ≈ 120 μm thickness due to the elasticity of the flexible electrodes, as shown in the Supplementary Material, figure S1. This materials consists of a thin, flexible and conductive activated carbon 'cloth' which does not require the use of a conventional current collector, such as nickel foam, Fig. 1. Electrodes can then be produced by punching a region of appropriate size and shape out of the activated carbon cloth, as discussed below.

For electrodes containing carbon black as an additive, the carbon black and activated carbon were added to a beaker with 5 ml ethanol, and then mixed using a magnetic stir bar on a hotplate at 50 °C until most of the ethanol had evaporated. The temperature was then reduced and the PTFE binder (5 wt% by total weight of electrode material) was added. From this point the method was the same as before. The method for producing electrodes using FLG directly mixed in as a conductive additive is similar to that for the carbon black additive, except that the FLG is suspended in water, so no ethanol is added in the initial stages.

To produce the vacuum infused FLG electrodes, a sheet of activated carbon cloth, produced by the same procedure as the activated carbon electrodes without additive, was placed in a vacuum filtration apparatus instead of a filter membrane. The desired quantity of FLG suspension was mixed with UHP water to a volume of 150 ml and infused into the activated carbon sheet. By varying the quantity of FLG suspension while retaining the same initial electrode mass, the composition of the electrodes could be varied. Electrodes remained flexible whichever conductive additive or route for addition was employed.

All electrodes, except those used to derive the Ragone plot (discussed later), were formed by punching the electrode 'cloth' into 15 mm diameter discs and their sheet resistance measured using a 4-point Van der Pauw method prior to electrochemical testing. The electrodes used to produce the Ragone plot were cut into 10 mm discs, to allow for higher currents to be applied during testing without overloading the potentiostats. Both the activated carbon 'cloth', and the carbon black-containing electrodes had total areal mass densities of 4.7 ± 0.9 mg cm^{-2}. As the FLG was then added to the activated carbon, the total areal mass densities of the electrodes varied from a comparable value of 4.24 ± 0.04 mg cm^{-2} for those containing approximately 5 wt% FLG, to 9.4 ± 0.8 mg cm^{-2} for those containing over 50 wt% FLG.

Free-standing FLG 'paper' was produced by filtering FLG suspension onto 0.4 μm pore cellulose nitrate membranes (Whatman) and washing with an excess of UHP water. The resulting film was dried at ambient temperature overnight before being peeled from the membrane.

2.3. Materials and electrode characterisation

Scanning electron microscopy (SEM) was carried out on all electrode types using a Zeiss Sigma 300 VP microscope using an incident beam energy of 3 keV and secondary electron detection. In addition, to determine the size distribution of the FLG platelets, small quantities of suspension were diluted in UHP water and filtered onto anodic alumina (AA) membranes (Anodisc). These were imaged using backscattered electrons with a primary beam energy of either 3.2 keV or 5 keV. Imaging of these samples was performed in variable pressure mode at ≤ 10 Pa to neutralise charge build up on the AA membranes. To obtain the platelet size distributions and account for their irregular shapes, the planar area of each FLG platelet was separately measured from a large number of SEM images for each centrifugation protocol.

The porosity of the activated carbon powder and FLG paper was measured using a Micromeritics Tri-star adsorption analyser at 77 K. Prior to measurements the sample was held under vacuum at 80 °C overnight, followed by 2 h at 300 °C in a nitrogen environment, in a Micromeritics Flowprep system. The Brunauer–Emmett–Teller (BET) equation was used for surface area determination, while Barrett–Joyner–Halenda (BJH) theory was used for pore size analysis. Raman spectroscopy was carried out on the FLG paper, activated carbon and electrode materials using an ASEQ Instruments RM1 Raman Spectrometer with a 532 nm green laser (Opto Engine LLC) operating at a

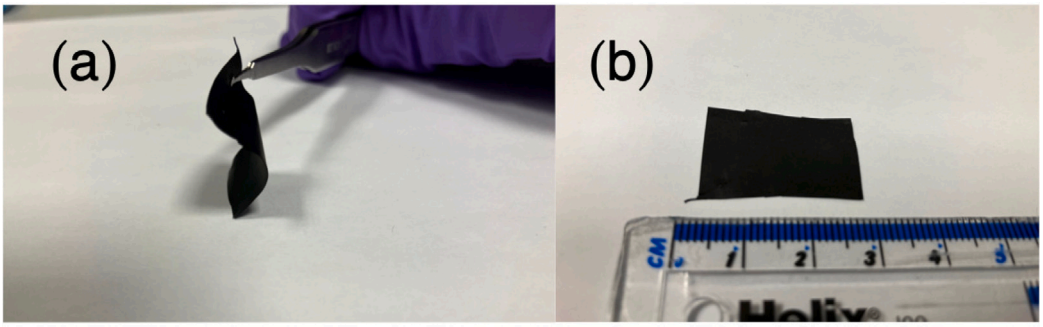

Fig. 1. Section cut from a typical piece of conductive activated carbon 'cloth': (a) under deformation and (b) after deformation.

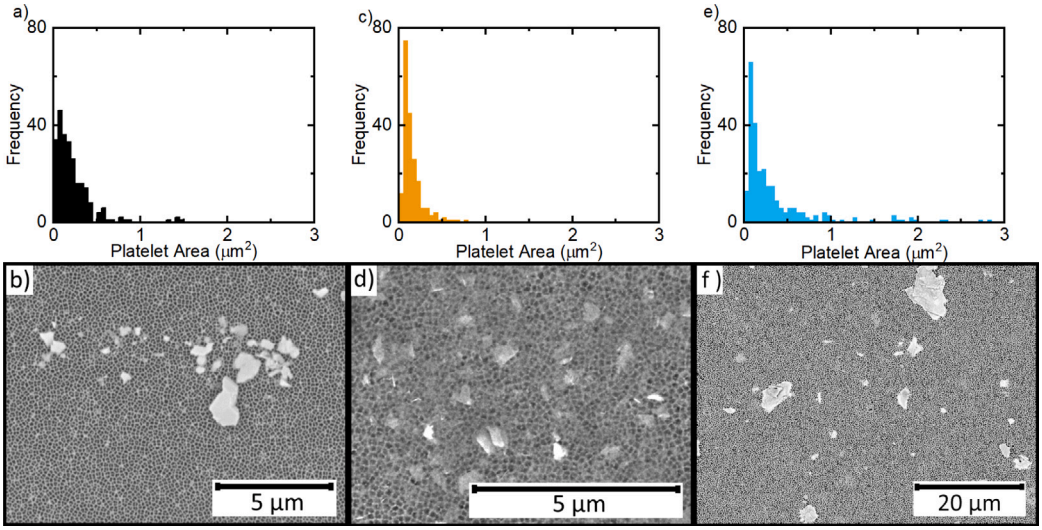

Fig. 2. FLG platelet size (planar area) distributions and typical SEM images obtained using backscattered electrons of platelets deposited on anodic alumina for the three centrifuging protocols used: (a,b) mFLG, (c,d) hFLG, and (e,f) uFLG.

beam power density of 15 W cm^{-2} at the sample surface, which was well below that at which damage is observed to occur. Raman peaks were fitted to Lorentzian functions using Fityk [20], and FLG platelet thicknesses calculated using the spectroscopic metrics developed by Backes and co-workers [21].

2.4. Electrochemical measurements

Electrochemical testing was undertaken using a home-built reusable spring loaded two-electrode cell. Glass fibre filter membranes (Sartorius), 25 mm diameter, were used as separators and 6M aqueous KOH was used as an electrolyte. Cyclic voltammetry (CV) and galvanostatic charge/discharge (GCD) were performed using either a homemade USB-controlled potentiostat, based on that described by Dobbelaere et al. [22] or a Palmsens 4 potentiostat. CV was performed for 25 cycles and the specific capacitance (C_{sp}) determined for each cycle from the area enclosed by the CV curve according to:

$$C_{sp} = \frac{4}{m}\frac{\oint i(t)dt}{\Delta V}$$

where m is the total mass of both electrodes, ΔV the potential window over which the CV cycle is measured and $i(t)$ is the instantaneously measured current, with the integral taken over each individual cycle.

GCD measurements were performed for 60 cycles, the specific capacitance determined from the slope of the linear part of the discharge region of the GCD curve. The voltage drop upon reversal of the cell current was used to determine equivalent series resistance (ESR). The (specific) energy density, E_{sp} is calculated from the linear region of the discharge part of the charge/discharge cycle from the formula:

$$E_{sp} = \frac{4}{m} \times i_d \int_{t(V_{min})}^{t(V_{max})} V(t)dt$$

where i_d is the discharge current, $t(V_{max})$ is the time at the start of the linear region of the discharge part of the cycle, $t(V_{min})$ time at the end of the linear region of the discharge cycle and $V(t)$ is the instantaneous potential at time t. The (average) power density is determined from the linear region of the discharge cycle by:

$$P_{sp} = E_{sp}/\Delta t$$

where Δt is the time over which the linear region of the discharge curve extends.

All C_{sp} values reported in this work are referenced to the *total* electrode mass, rather than that of the active materials or additives alone and so reflect the 'real world' electrode performance. Cycle life measurements involved measuring the capacity retention from GCD over 5000 charge/discharge cycles.

3. Results and discussion

The specific surface area (SSA) and pore size distributions (PSD) of the activated carbon and FLG used to construct EDLC electrodes were determined from N_2 adsorption/desorption isotherms (figure S2, Supplementary Material) and are reported in Table 1. The activated carbon material displays a type IV isotherm (figure S2 (a)), which is indicative of a hierarchical pore structure. The significant intake

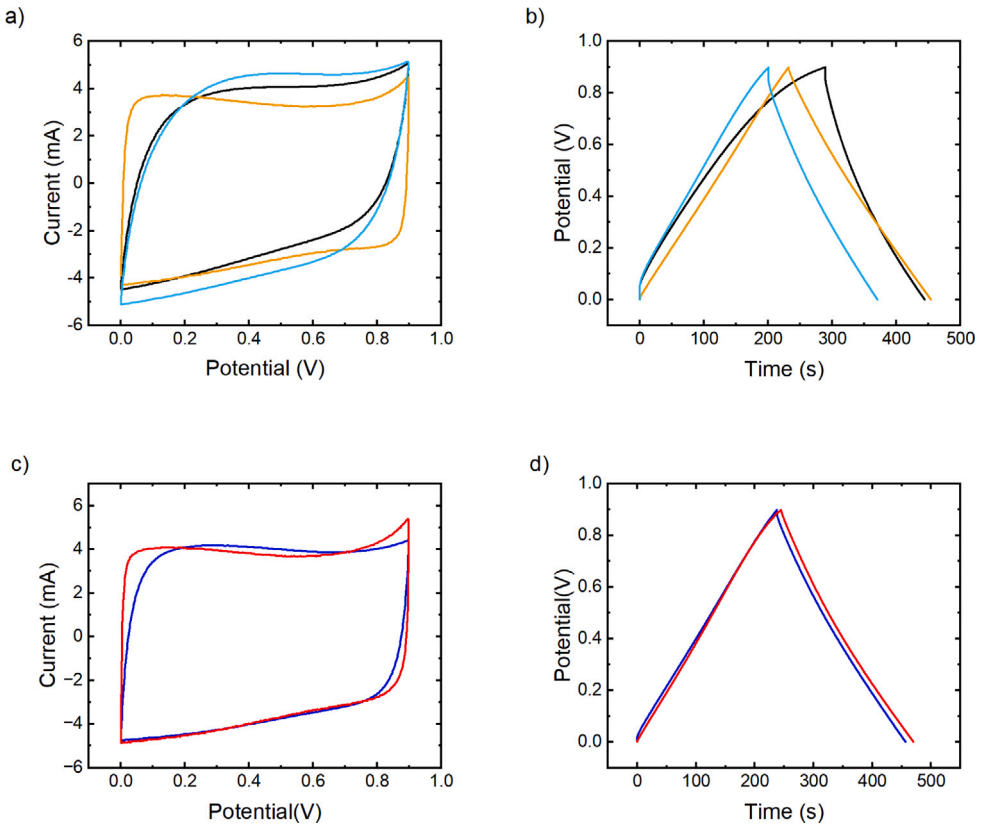

Fig. 3. (a,c) Cyclic voltammograms obtained at a voltage sweep rate of 10 mV s^{-1}, and (b,d) GCD curves obtained at a specific current of 0.1 A g^{-1}, of activated carbon electrodes (black a,b), electrodes with 5 wt% carbon black (orange a,b), and electrodes with 5 wt% uFLG directly mixed in (light blue a,b), electrodes with 5 wt% uFLG mixed in, which have subsequently been washed (dark blue c,d), and electrodes with 5 wt% uFLG added by vacuum infiltration (red c,d). (For interpretation of the references to colour in this figure legend, the reader is referred to the web version of this article.)

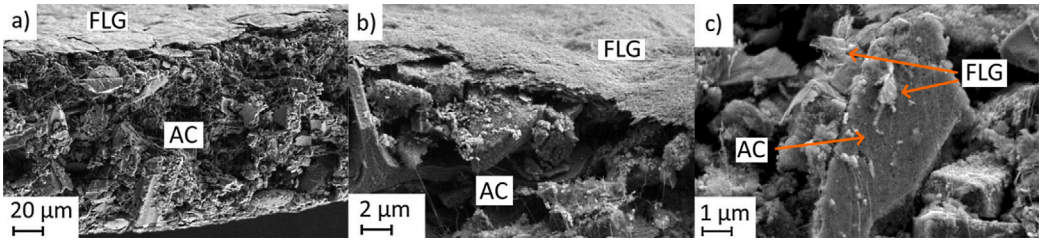

Fig. 4. SEM images showing; (a) a cross section of a typical electrode with vacuum infiltrated FLG additive; (b) a magnified image showing the FLG layer on the back of the electrode; (c) magnified image showing FLG platelets deposited on an activated carbon particle (indicated with arrows).

of N_2 at low relative pressures corresponds to capillary condensation and consequently indicates microporosity, with a hysteresis loop at higher pressure indicating the presence of mesoporosity [23]. The FLG sample (figure S2 (c)), in contrast, shows a type V isotherm, indicating a mesoporous pore structure with an absence of microporosity. The SSA of the activated carbon is in the typical range observed for such material [24]. However, the SSA of few-layer graphene, obtained from a vacuum filtered film, is much smaller than that which would be expected from isolated few-layer graphene platelets and is indicative of considerable re-stacking of the FLG in the absence of an external 'scaffold', which is also reflected in cross-sectional SEM micrographs of the FLG paper (figure S3, Supplementary Material).

Size (planar area) distributions of the few-layer graphene platelets are given by the histograms in Fig. 2(a,c,e) determined from multiple SEM images, examples of which shown in Fig. 2(b,d,f). The highly centrifuged material consists largely of graphene platelets of small lateral size, while the moderately centrifuged and uncentrifuged material contain both small platelets and a number of significantly larger platelets. The histograms also show the narrow size distribution of the highly centrifuged material, with a mean platelet area of 0.18 ± 0.02 μm^2 (where the error quoted is the standard error in the mean) and a standard deviation of 0.4 μm^2, while the moderately centrifuged and uncentrifuged materials have broader size distributions with mean platelet sizes of 0.5 ± 0.2 μm^2 and 1.3 ± 0.6 μm^2, and standard deviations of 3 μm^2 and 10 μm^2, respectively. The large standard deviations are caused by the data following an asymmetric distribution.

Table 1
Specific surface area (SSA), total pore volume (V_{total}), and average pore diameter (D_{av}) for the activated carbon and FLG materials.

Sample	SSA (m^2 g^{-1})	V_{total} (cm^3 g^{-1})	D_{av} (nm)
Activated carbon	870	0.73	3.4
Few-layer graphene	13	0.141	44

Raman spectroscopy (figure S4, Supplementary Material) shows that the ratio between the intensities of the D and D' peaks, $I_D/I_{D'}$ increased from 2 ± 1 for the as-supplied graphite flakes to 7 ± 1,

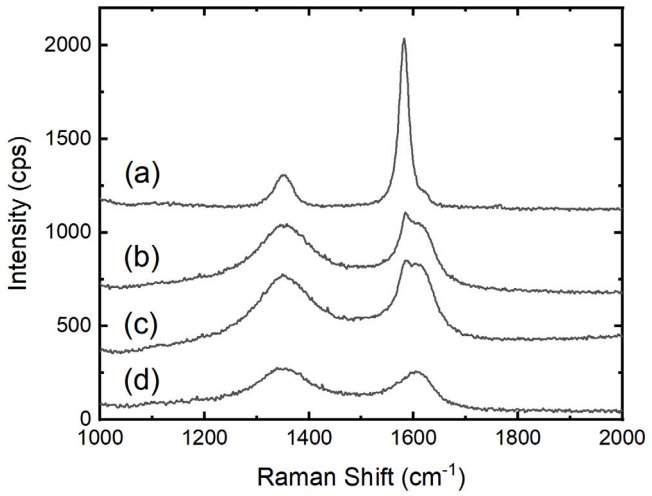

Fig. 5. Raman spectra showing the *D* and *G* band region for (a) FLG, (b) the 'graphene-rich' side of a FLG-infused activated carbon electrode, (c) the 'graphene-poor' side of a FLG-infused activated carbon electrode and (d) a standard electrode made with AC.

Table 2
Mean values of specific capacitance (C_{sp}), equivalent series resistance (ESR), and sheet resistance data for a variety of activated carbon (AC) electrodes with carbon black (CB) or FLG conductive additives. The C_{sp} and ESR values were derived from CV at 10 mV s^{-1} and GCD at 0.1 A g^{-1} measured over a potential window of 0.9 V. The mean and standard errors are derived from multiple cells measured for each electrode type.

Sample	C_{sp} from CV (F g^{-1})	ESR from GCD (Ω)	C_{sp} from GCD (F g^{-1})	Sheet resistance (Ω □$^{-1}$)
AC	52 ± 5	35 ± 9	73.6 ± 0.1	5800 ± 500
AC + 5% CB	95.49 ± 0.03	2.22 ± 0.02	99.7 ± 0.1	1700 ± 90
AC + 5% FLG (uncentrifuged, mixed)	53 ± 8	19 ± 8	77.5 ± 0.8	3700 ± 100
AC + 5% FLG (uncentrifuged, mixed & washed)	81 ± 6	10 ± 4	89 ± 5	2800 ± 200
AC + 5% FLG (uncentrifuged, vacuum filtered)	102.9 ± 0.1	1.4 ± 0.1	99.06 ± 0.03	1700 ± 60

characteristic of a transition from domination by boundary-like defects to vacancy-like defects [25]. Using the spectroscopic metrics developed by Backes et al. [21], the average platelet thickness was calculated to be 4±1.5 graphene layers, whichever centrifuging protocol was employed, confirming the material to be few-layer graphene.

Fig. 3 shows typical cyclic voltammograms measured at a voltage sweep rate of 10 mV s^{-1} (a), and GCD curves measured at 0.1 A g^{-1} (b) of activated carbon electrodes produced without conductive additive (black curve), 5 wt% Timcal C65 (orange curve), and 5 wt% uFLG directly mixed from suspension with activated carbon (blue curve). Initial electrode characterisation was carried out over a voltage window, ΔV, of 0.9 V, well below the threshold for water splitting and hence electrolyte degradation [26] to ensure good stability for comparative measurements of C_{sp} and ESR. The limited efficacy of the uFLG directly mixed into the activated carbon electrodes as a conductive additive is reflected in the relatively small area enclosed by the CV curve and large voltage drop visible in GCD. Table 2 shows mean values of C_{sp} and ESR derived from multiple CV and GCD curves obtained from several cells. It can be seen that direct mixing of uFLG into the activated carbon electrodes leads to only a modest improvement in cell metrics, with both C_{sp} and ESR values comparing poorly with those of electrodes containing 5 % carbon black.

The mediocre behaviour of electrodes produced by directly mixing uFLG with activated carbon can be attributed to the presence of Triton X-100. This surfactant, which is required to ensure that the FLG remains in suspension, assembles at the water/FLG interface potentially presenting a barrier to conduction and blocking access to both the few-layer graphene and activated carbon surface area when the FLG is incorporated into the electrode. The latter effect is demonstrated by the improvement when electrodes produced by direct mixing of the uFLG suspension are subsequently washed with 500 ml of UHP water, as shown by the CV and GCD curves in Fig. 3(c, d) and the data in Table 2. After washing, the C_{sp}, measured by GCD at 0.1 A g^{-1}, increases from 77.5 ± 0.8 to 89 ± 5 F g^{-1}, which is closer to that of the electrodes produced with carbon black. This increase in specific capacitance most likely arises from an enhancement in the surface area accessible to ions after the removal of the surfactant. However, despite the improvement in specific capacitance, the ESR remains relatively high and hence direct mixing of 5 % uFLG produces an inferior electrode material to that produced by the same loading of carbon black. We attribute the high ESR of electrodes produced from uFLG by mixing and subsequent washing to poor contact between activated carbon and FLG. Removal of the surfactant increases the surface area accessible to ions but does not lead to structural re-arrangement improving contact between the additive and the active material.

In order to overcome the poor performance of FLG additive when directly mixed with the electrode precursors, we employed the novel approach of infusing uFLG into pre-formed activated carbon electrodes in an excess of UHP water by vacuum infiltration. Fig. 4 shows SEM images of typical vacuum infiltrated electrodes. The interior of the electrode is shown to be composed of activated carbon particles of a wide range of shapes and sizes, with the strands of PTFE binder clearly visible. The FLG material is also visible as a layered material on top of the electrodes (the layer of re-stacked FLG sheets is more clearly shown in Fig. 4(b)). Fig. 4(c) shows FLG platelets deposited on a grain of activated carbon in the body of the electrode. Further evidence of the successful infiltration of FLG throughout the activated carbon electrodes is provided by the Raman spectra presented in Fig. 5. Electrodes formed from activated carbon without additives present the typical features of amorphous carbons, with a broad *D* band at ≈ 1350 cm^{-1} and *G* band at ≈ 1600 cm^{-1}, Fig. 5(d). Upon infiltration of FLG the Raman spectra obtained from both the 'upper' and 'lower' faces (referring to orientation within the vacuum filtration apparatus) of the infiltrated electrodes, Figs. 5(b) and (c) respectively, consist of a superposition of spectra from the pure activated carbon electrode and FLG 'paper' (Fig. 5(a)). The superposition is particularly apparent when examining the *G* band of the FLG-infused electrode, where a sharp feature, corresponding to the narrow FLG *G* band at ≈ 1581 cm^{-1}, can be seen on the low energy side of the peak. The contribution of the FLG to the Raman spectra of the infused electrode is stronger on the upper surface of the electrode, upon which a continuous FLG film forms (Fig. 5(b)), however, this feature is also clearly present in spectra from the lower surface (Fig. 5(c)) indicating that FLG has infused throughout the body of the electrode, consistent with SEM observations.

Enhanced electrochemical function of the uFLG infiltrated electrodes is readily apparent from the CV and GCD plots shown in Fig. 3(c,d) obtained from samples with 5 wt% uFLG. The C_{sp} of the uFLG 'infused' electrodes is found to increase to 102.9 ± 0.1 F g^{-1} measured by CV and 99.06±0.03 F g^{-1} from GCD, similar to that found for the 5 wt% carbon black electrodes, and the ESR decreases to 1.4 ± 0.1 Ω. This improvement is reflected in an electrode sheet resistance which agrees with that of the carbon black containing electrodes within experimental error. The small size of the FLG platelets seen in Figs. 2 and 4 means it is difficult to discern the exact quantity and distribution of them in the body of the electrode material. However, the observation of a clear Raman signal from FLG on both sides of the electrodes (Fig. 5)

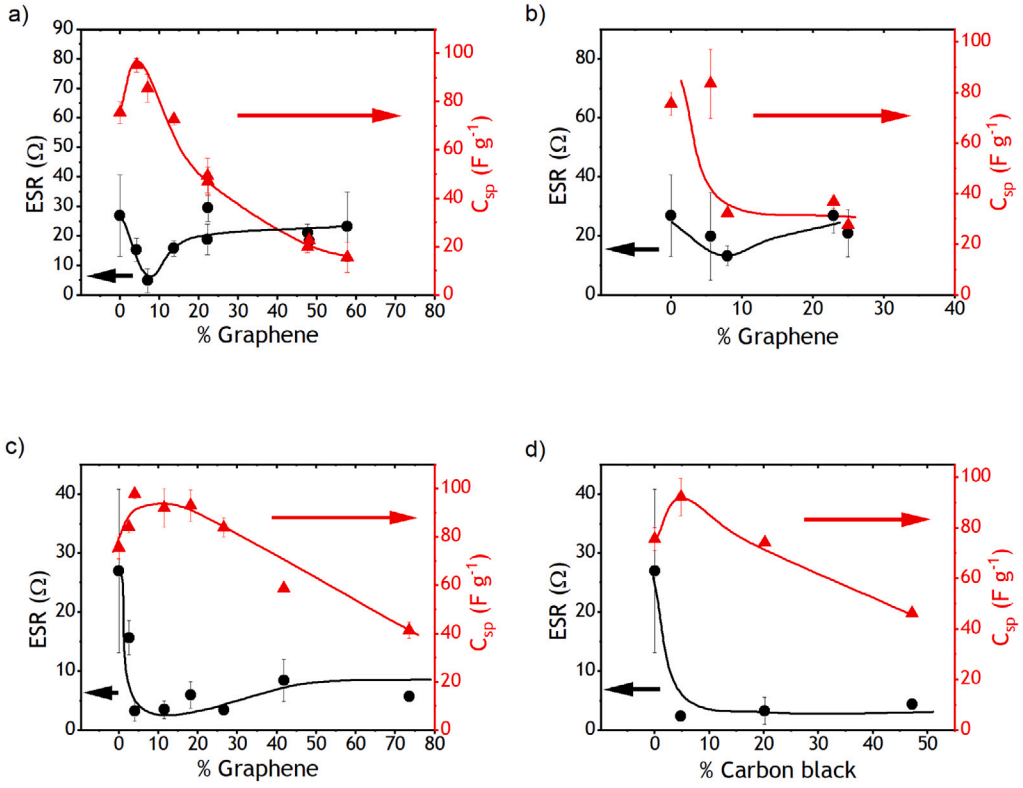

Fig. 6. Mean values of C_{sp} (red triangles) and ESR (black circles), derived from GCD at 0.1 A g^{-1} over a voltage window of 0.9 V, for varying quantities of: (a) moderately centrifuged FLG, (b) highly centrifuged FLG, and (c) uncentrifuged FLG, inserted by vacuum infiltration, and (d) varying levels of conventional carbon black conductive additive. The lines are a guide to the eye. (For interpretation of the references to colour in this figure legend, the reader is referred to the web version of this article.)

and the considerable decrease in electrode resistance, which cannot solely be attributed to a reduction of resistance between electrodes and contacts, implies that enough platelets must penetrate the bulk of the electrode to significantly improve conductivity. We can therefore conclude that, when incorporated into an activated carbon electrode through a route which is effective in removing surfactant, the FLG serves as an efficient conductive additive.

In order to determine the extent to which the FLG size distribution and loading influenced the effectiveness of FLG-infiltrated activated carbon electrodes, full electrochemical characterisation was performed on electrodes infiltrated with mFLG, hFLG and uFLG over a broad range of loading, Fig. 6(a-c). To provide a baseline to evaluate the effectiveness of the different FLG size distributions, a series of similar measurements was performed on samples in which the carbon black loading was similarly varied, Fig. 6(d).

Fig. 6(a) shows how C_{sp} and ESR varied with mFLG loading. Performance is optimised at 7 wt% mFLG, with a C_{sp} derived from CV of 82 ± 9 F g^{-1}, and C_{sp} and ESR derived from GCD of 86 ± 6 F g^{-1} and 5 ± 4 Ω, respectively. As the quantity of mFLG is increased the specific capacitance was found to decrease sharply to 11.9 F g^{-1} at 58 wt% mFLG. This is to be expected; as shown in the SEM image in Fig. 4, a significant amount of FLG stacks up on the back of the electrode which adds mass without significantly contributing to the electrode specific capacitance, due to FLG restacking. This behaviour could be expected to lead to a linear decrease in capacitance, which the measured data significantly diverges from, instead falling off steeply at first, then more gently at higher concentrations. More unusual behaviour is observed in the ESR: although there is an improvement with loading to around 7 wt% FLG, as the amount of mFLG increases further, the ESR also increases before plateauing at around 20 Ω. This is in sharp contrast to sheet resistance measurements (not shown), which show a monotonic decrease in electrode resistance as the mFLG loading increases, due to the graphene forming a high conductivity layer on the back of the electrode, which means that the sheet resistance cannot be directly related to the ESR associated with a cell produced from the electrode material.

The effectiveness of hFLG as a function of loading is presented in Fig. 6(b). Compared with those incorporating mFLG, the samples show a similar or decreased performance across all mass loadings. The results of electrochemical analysis of electrodes loaded with varying percentages of uFLG are shown in Fig. 6(c). Performance is optimised at approximately 4–20 wt% uFLG loading, a wider range of loading compared with the other materials. Moreover, the ESR, after dropping rapidly, remains low with increased mass loading unlike the variation observed for the mFLG additive. C_{sp} (derived from GCD) remains above 90 F g^{-1} up to 20 wt% uFLG, before decreasing slowly. This behaviour is also superior to that observed for commercial carbon black conductive additive (Fig. 6(d)). A similar trend in ESR and C_{sp} is observed for both carbon black and uFLG with the peak value of C_{sp} slightly lower in the former case and decreasing with loading above 5 wt%.

As described above, initial electrode characterisation was carried out over a limited voltage window of 0.9 V, however, maximum energy and power density is obtained from the widest possible voltage window compatible with long-term device stability. Hence, the cycle stability of electrodes produced with the optimal combination of FLG size distribution and loading (4–20 wt% vacuum infiltrated uFLG) was tested over 5000 charge/discharge cycles at increasing voltage windows and compared with a 'standard' device containing 5 wt% carbon black.

Fig. 7 compares the stability of devices produced from carbon black (orange line) and 5 wt% uFLG (black line) over a voltage window of (a) 1.2 V and (b) 1.4 V at a specific current of 1 A g^{-1}. Both display excellent stability, with discharge capacitance increasing over 5000 cycles at 1.2 V, and remaining close to 95 % after 5000 cycles at 1.4 V. For both potentials, the FLG-containing device shows marginally better capacity retention; 105 % compared with 103 % for the carbon black loaded electrodes at 1.2 V, and 97 % compared with 94 % at

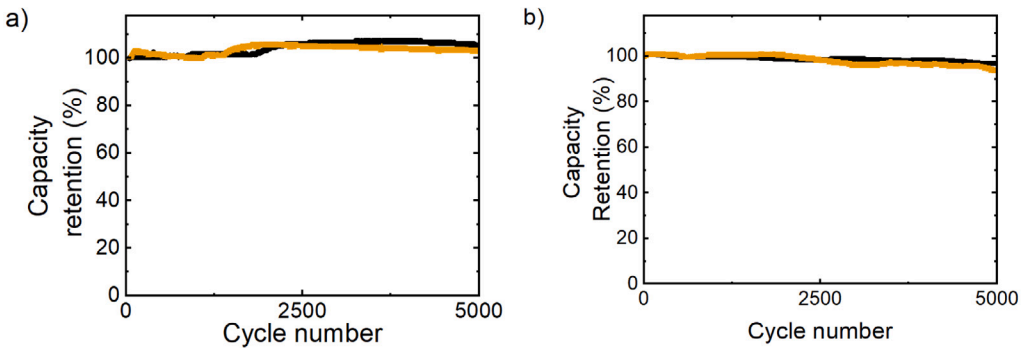

Fig. 7. Discharge capacity retention over 5000 cycles of galvanostatic charge/discharge with a current density of 1 A g^{-1}. (a) data obtained with a potential window of 1.2 V and (b) 1.4 V. In both figures, data from devices with electrodes containing 5 wt% vacuum infiltrated uncentrifuged FLG is shown in black, and data from devices with electrodes containing 5 wt% carbon black is shown in orange. (For interpretation of the references to colour in this figure legend, the reader is referred to the web version of this article.)

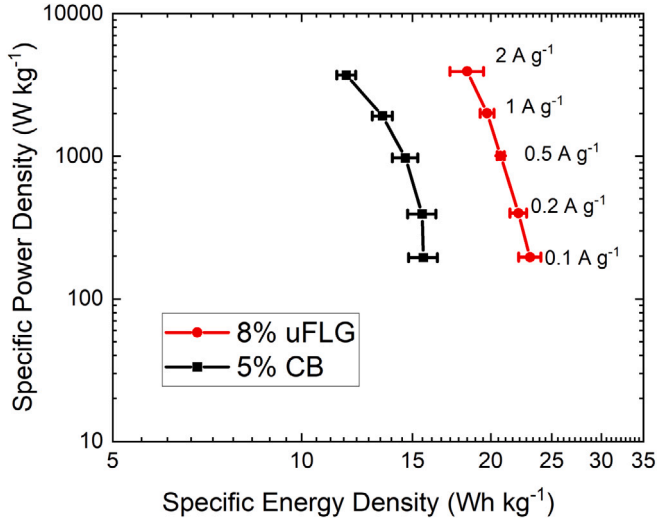

Fig. 8. Ragone plot comparing performance of activated carbon electrodes with 8 wt% vacuum infiltrated uFLG (red circles and line) with electrodes containing 5% carbon black (black squares and line). Power and energy density are derived from GCD data collected between 0.1 and 2 A g^{-1} over a window of 1.2 V. Each data set is the mean from three different cells. Error bars are the standard error in the mean. (For interpretation of the references to colour in this figure legend, the reader is referred to the web version of this article.)

1.4 V, although the differences between materials is within our typical reproducibility error and so cannot be considered as significant. Given the slow decrease in capacity with cycling using the 1.4 V voltage window and difficulty in fully charging over this window at very low specific currents ($\lesssim$ 0.2 A g^{-1}) we can draw the conclusion that the optimum potential window for both devices is 1.2 V.

Fig. 8 shows a Ragone plot for electrodes with 8 wt% vacuum infiltrated uFLG conductive additive and 5 wt% carbon black additive (within the optimum loading range for each material) over a 1.2 V potential window. From the data it can be seen that the FLG devices show a greater energy density across the full range of power densities tested. Both reproducibility and the breadth of the optimal uFLG weight loading compared with that of the carbon black are demonstrated in figure S5 of the Supplementary Material. The energy storage for both EDLCs was optimised at a power density of around 200 W kg^{-1}, corresponding to a specific energy of 23 $\pm$ 1 Wh kg^{-1} for the uFLG device, and 15.9 $\pm$ 0.9 Wh kg^{-1} for the carbon black device, a 48 $\pm$ 9% performance improvement when using uFLG compared with carbon black. This arises due to uFLG-infiltrated devices having a higher C_{sp} of 142.3$\pm$0.1 F g^{-1} over the 1.2 V window, compared with 96.81$\pm$0.02 F g^{-1} for the devices with carbon black additive. The ESRs of the uFLG and carbon black-containing EDLCs were found to be comparable at 1.3$\pm$0.4 Ω and 3$\pm$1 Ω, respectively, resulting in similar power densities at a given specific current draw. Over the range of specific currents tested (0.1 A g^{-1} to 2 A g^{-1}) the energy density of the electrodes with 8 wt% uFLG loading was on average 47 $\pm$ 3% higher than that of electrodes with 5 wt% carbon black loading at comparable specific power densities (figure S6, Supplementary Material). The gain in C_{sp} observed for optimal uFLG loading in comparison with that for optimal carbon black loading indicates that the improved performance of uFLG-infiltrated electrodes compared with those produced with carbon black arises from an *active* contribution of the uFLG to the double layer capacitance.

4. Conclusions

Few-layer graphene produced by an environmentally benign approach using high shear exfoliation into a surfactant-stabilised aqueous suspension has been investigated as a conductive additive for aqueous supercapacitors using activated carbon electrodes. Three different centrifuging protocols were adopted to produce FLG suspensions with differing lateral size distributions: mFLG, hFLG and uFLG. Raman spectroscopy-based metrics determined that the average thickness of the FLG platelets was 4 $\pm$ 1.5 graphene layers, independent of centrifuging protocol.

Direct mixing of FLG into the electrode material showed poor performance compared with a commercially available carbon black additive. Specific capacitance was improved slightly by washing the electrodes, implying that Triton X-100 left over from the shear exfoliation process may have reduced access to pores within the activated carbon. However, ESR remained high for direct mixing of FLG even after washing.

Based on these results, a novel vacuum infiltration approach was developed. mFLG-infiltrated electrodes performed well at a 7 wt% concentration, but counter-intuitively, the series resistance increased above this concentration, while hFLG, with a smaller average platelet dimension, performed poorly across all concentrations tested. In contrast, uncentrifuged uFLG-infiltrated electrodes performed well over a broad range of mass loadings, retaining a specific capacitance of over 90 F g^{-1} and low ESR at concentrations between 4 and 20 wt%.

Electrodes containing 4–8 wt% uFLG were compared with those containing 5 wt% commercial carbon black, and were found to have a substantially improved (by $\approx$ 50%) specific energy density when measured at comparable power densities. Power densities at a given specific current draw were similar for electrodes made with the two conductive additives, reflecting similar cell ESRs and the materials possessed comparable cyclability over an optimised potential window of 1.2 V. These results demonstrate that high-shear exfoliated FLG, with no subsequent centrifuging treatment, performs significantly better than commercially-available carbon black as a conductive additive

for activated carbon electrodes used in aqueous EDLCs, if introduced into activated carbon electrodes by our novel infiltration technique. Moreover, our approach is generalisable to any two-dimensional solid or nanomaterial which can be produced in a surfactant-stabilised suspension, opening the route to the exploration of a broad range of electrode compositions.

CRediT authorship contribution statement

R.E. Williams: Methodology, Investigation, Formal analysis, Writing – original draft. **S. Sukumaran:** Investigation. **Q. Abbas:** Investigation, Writing – review & editing. **M.R.C. Hunt:** Conceptualisation, Investigation, Writing – review & editing, Supervision, Funding acquisition.

Declaration of competing interest

The authors declare that they have no known competing financial interests or personal relationships that could have appeared to influence the work reported in this paper.

Acknowledgement

This work was supported by the United Kingdom Engineering and Physical Sciences Research Council (Grants EP/S023836/1 and EP/R021503/1).

Appendix A. Supplementary data

Supplementary material related to this article can be found online at https://doi.org/10.1016/j.carbon.2023.118744.

References

[1] A.G. Pandolfo, A.F. Hollenkamp, Carbon properties and their role in supercapacitors, J. Power Sources 157 (1) (2006) 11–27.
[2] A. Berrueta, A. Ursúa, I.S. Martín, A. Eftekhari, P. Sanchis, Supercapacitors: Electrical characteristics, modeling, applications, and future trends, IEEE Access 7 (2019) 50869–50896, http://dx.doi.org/10.1109/ACCESS.2019.2908558.
[3] P. Simon, Y. Gogotsi, Materials for electrochemical capacitors, Nature Mater. 7 (2008) 845–854.
[4] M. Mirzaeian, Q. Abbas, A. Ogwu, P. Hall, M. Goldin, M. Mirzaeian, H.F. Jirandehi, Electrode and electrolyte materials for electrochemical capacitors, Int. J. Hydrogen Energy 42 (40) (2017) 25565–25587.
[5] P.J. Hall, M. Mirzaeian, S.I. Fletcher, F.B. Sillars, A.J.R. Rennie, G.O. Shitta-Bey, G. Wilson, A. Cruden, R. Carter, Energy storage in electrochemical capacitors: designing functional materials to improve performance, Energy Environ. Sci. 3 (9) (2010) 1238–1251.
[6] A. González, E. Goikolea, J.A. Barrena, R. Mysyk, Review on supercapacitors: Technologies and materials, Renew. Sustain. Energy Rev. 58 (2016) 1189–1206.
[7] G. Wang, Z. Shao, Z. Yu, Comparisons of different carbon conductive additives on the electrochemical performance of activated carbon, Nanotechnology 18 (20) (2007) 205705.
[8] E.A. Kiseleva, S.A. Kochanova, E.J. Shkolnikov, A.B. Tarasenko, O.V. Zaitseva, O.V. Uryupina, G.V. Valyano, M.A. Zhurilova, Influence of carbon conductive additives on electrochemical double-layer supercapacitor parameters, IOP Conf. Ser. J. Phys. Conf. Ser. 946 (2018).
[9] N. Jäckel, D. Weingarth, M. Zeiger, M. Aslan, I. Grobelsek, V. Presser, Comparison of carbon onions and carbon blacks as conductive additives for carbon supercapacitors in organic electrolytes, J. Power Sources 272 (2014) 1122–1133.
[10] A.G. Pandolfo, G.J. Wilson, T.D. Huynh, A.F. Hollenkamp, The influence of conductive additives and inter-particle voids in carbon EDLC electrodes, Fuel Cells 10 (5) (2010) 856–864.
[11] A.D. Maynard, Are we ready for spray-on carbon nanotubes? Nature Nanotechnol. 11 (6) (2016) 490–491.
[12] M.D. Stoller, S. Park, Y. Zhu, J. An, R.S. Ruoff, Graphene-based ultracapacitors, Nano Lett. 8 (10) (2008) 3498–3502.
[13] R. Wang, Y. Qian, W. Li, S. Zhu, F. Liu, Y. Guo, M. Chen, Q. Li, L. Liu, Performance-enhanced activated carbon electrodes for supercapacitors combining both graphene-modified current collectors and graphene conductive additive, Materials 11 (2018) 799.
[14] Y. Niu, J. Wang, J. Zhang, Z. Shi, Graphene quantum dots as a novel conductive additive to improve the capacitive performance for supercapacitors, J. Electroanal. Soc. 828 (2018) 1–10.
[15] B. Xu, H. Wang, Q. Zhu, N. Sun, B. Anasori, L. Hu, F. Wang, Y. Guan, Y. Gogotsi, Reduced graphene oxide as a multi-functional conductive binder for supercapacitor electrodes, Energy Storage Mater. 12 (2018) 128–136.
[16] K.R. Paton, E. Varrla, C. Backes, R.J. Smith, U. Khan, A. O'Neill, C. Boland, M. Lotya, O.M. Istrate, P. King, T. Higgins, S. Barwich, P. May, P. Puczkarski, I. Ahmed, M. Moebius, H. Pettersson, E. Long, J. Coelho, S.E. O'Brien, E.K. McGuire, B.M. Sanchez, G.S. Duesberg, N. McEvoy, T.J. Pennycook, C. Downing, A. Crossley, V. Nicolosi, J.N. Coleman, Scalable production of large quantities of defect-free few-layer graphene by shear exfoliation in liquids, Nature Mater. 13 (6) (2014) 624–630.
[17] J.N. Coleman, Liquid exfoliation of defect-free graphene, Acc. Chem. Res. 46 (1) (2013) 14–22.
[18] E. Varrla, K.R. Paton, C. Backes, A. Harvey, R.J. Smith, J. McCauley, J.N. Coleman, Turbulence-assisted shear exfoliation of graphene using household detergent and a kitchen blender, Nanoscale 6 (20) (2014) 11810–11819.
[19] R. Raccichini, A. Varzi, S. Passerini, B. Scrosati, The role of graphene for electrochemical energy storage, Nature Mater. 14 (3) (2015) 271–279.
[20] M. Wojdyr, *Fityk*: a general-purpose peak fitting program, J. Appl. Crystallogr. 43 (5 Part 1) (2010) 1126–1128.
[21] C. Backes, K.R. Paton, D. Hanlon, S. Yuan, M.I. Katsnelson, J. Houston, R.J. Smith, D. McCloskey, J.F. Donegan, J.N. Coleman, Spectroscopic metrics allow in situ measurement of mean size and thickness of liquid-exfoliated few-layer graphene nanosheets, Nanoscale 8 (7) (2016) 4311–4323.
[22] T. Dobbelaere, P.M. Vereecken, C. Detavernier, A USb-controlled potentiostat/galvanostat for thin-film battery characterization, HardwareX 2 (2017) 34–49.
[23] K.V. Kumar, S. Gadipelli, B. Wood, K.A. Ramisetty, A.A. Stewart, C.A. Howard, D.J.L. Brett, F. Rodriguez-Reinoso, Characterization of the adsorption site energies and heterogeneous surfaces of porous materials, J. Mater. Chem. A 7 (2019) 10104–10137.
[24] L. Wei, G. Yushin, Nanostructured activated carbons from natural precursors for electrical double layer capacitors, Nano Energy 1 (4) (2012) 552–565.
[25] A. Eckmann, A. Felten, A. Mishchenko, L. Britnell, R. Krupke, K.S. Novoselov, C. Casiraghi, Probing the nature of defects in graphene by raman spectroscopy, Nano Lett. 12 (8) (2012) 3925–3930.
[26] X. Zang, C. Shen, M. Sanghadasa, L. Lin, High-voltage supercapacitors based on aqueous electrolytes, ChemElectroChem 6 (4) (2019) 976–988.